

Metal clusters with hidden ground states: Melting and structural transitions in Al_{115}^+ , Al_{116}^+ , and Al_{117}^+

Baopeng Cao, Anne K. Starace, Oscar H. Judd, Indrani Bhattacharyya, and Martin F. Jarrold^{a)}

Department of Chemistry, Indiana University, 800 East Kirkwood Ave., Bloomington, Indiana 47405, USA

(Received 9 June 2009; accepted 17 August 2009; published online 23 September 2009)

Heat capacities measured as a function of temperature for Al_{115}^+ , Al_{116}^+ , and Al_{117}^+ show two well-resolved peaks, at around 450 and 600 K. After being annealed to 523 K (a temperature between the two peaks) or to 773 K (well above both peaks), the high temperature peak remains unchanged but the low temperature peak disappears. After considering the possible explanations, the low temperature peak is attributed to a structural transition and the high temperature peak to the melting of the higher enthalpy structure generated by the structural transition. The annealing results show that the liquid clusters freeze exclusively into the higher enthalpy structure and that the lower enthalpy structure is not accessible from the higher enthalpy one on the timescale of the experiments. We suggest that the low enthalpy structure observed before annealing results from epitaxy, where the smaller clusters act as a nucleus and follow a growth pattern that provides access to the low enthalpy structure. The solid-to-solid transition that leads to the low temperature peak in the heat capacity does not occur under equilibrium but requires a superheated solid.

© 2009 American Institute of Physics. [doi:10.1063/1.3224124]

I. INTRODUCTION

The melting transitions of isolated metal nanoclusters have received a lot of attention recently. Well-defined melting transitions have been observed for metal clusters with fewer than 100 atoms. In this size regime, adding or subtracting a single atom can change the melting temperature dramatically. Experimental studies have now been performed for a variety of cluster materials including sodium,^{1–8} tin,^{9,10} gallium,^{11–13} sodium chloride,¹⁴ and aluminum,^{15–19} and these measurements have stimulated a number of theoretical studies.^{20–24}

Most of the experimental studies have employed heat capacity measurements to identify the melting transitions. Here, the signature of melting is a peak in the heat capacity due to the latent heat. In simulations, there are a number of examples where two peaks have been observed in the heat capacity.^{25–34} This behavior is usually called premelting when the low temperature peak is the smaller of the two and postmelting when the higher temperature peak is the smaller. However, multiple peaks have rarely been seen in the experimental studies. A few examples of premelting (Al_{51}^+ and Al_{52}^+)¹⁵ and postmelting (Al_{61}^+ and Al_{83}^+)¹⁷ have been reported for aluminum clusters. Postmelting has also been reported for Na_{147}^+ .³⁵ However, in all of these examples, the second peak is just a shoulder on the main peak. There have been no experimental results reported with the well-separated peaks seen in some of the simulations. In this manuscript we report the observation of two well-resolved peaks in the heat capacities of Al_{115}^+ , Al_{116}^+ , and Al_{117}^+ clusters. Annealing studies were performed to shed light on the origin of the peaks.

A number of recent simulations have shown that cluster melting can be preceded by structural transitions.^{36–43} For example, using a Gupta potential, Li *et al.* found that structural transitions between low enthalpy geometries (the ground state, icosahedral, and cuboctahedral) occur for Au_{55} at temperatures well below the melting temperature.³⁹ Cleveland *et al.* found that for Au_{146} and Au_{459} the melting process is punctuated by solid-to-solid structural transformations from the ground state to higher enthalpy icosahedral structures which are precursors to melting.³⁷ Schebarchov and Handy discovered that structural transitions occur in the solid part of a coexisting solid-liquid Ni_{1415} cluster.⁴⁰ In the case of palladium clusters, transitions from both fcc and decahedral ground states to icosahedral structures precede melting.⁴³ The transitions emerge during solid-liquid phase coexistence and appear to occur through fluctuations in the molten fraction and subsequent recrystallization into the icosahedral structure. According to Zhang *et al.*, a cuboctahedral to icosahedral structural transition occurs for nickel clusters with 309 atoms before the solid-to-liquid transition. However, for larger clusters (561, 923, 1415, and 2057 atoms) the cuboctahedral and icosahedral geometries melt (at slightly different temperatures) without undergoing structural transitions.⁴²

Solid-solid structural transitions are frequently found to precede melting for Lennard-Jones (LJ) clusters, resulting in two well-resolved peaks in heat capacity.^{44–50} For example, using exchange Monte Carlo simulations Mandelshtam *et al.* found that LJ_n clusters with $n=74–78$ have two peaks in their heat capacities.⁴⁶ The peak at higher temperatures is attributed to a melting transition, and the lower temperature peak is assigned to a solid-to-solid structural transition from the decahedral ground state to an icosahedral geometry.

^{a)}Electronic mail: mfj@indiana.edu.

Noya and Doye found that structural transitions precede melting in LJ_{309} .⁴⁷ The ground state of this cluster is a complete Mackay icosahedron, and so this finding breaks the paradigm that multiple peaks in heat capacity are observed for clusters with incomplete geometric shells. In the case of LJ_{309} , the main structural transition is similar to surface roughening and leads to the formation of pits and islands on the cluster surface.

Most of the experimental studies of structural transitions are for supported nanoclusters.^{51,52} For example, using high-resolution electron microscopy, Koga *et al.* found that gold nanoparticles (3–14 nm in diameter) undergo a structural transformation from icosahedral to a decahedral morphology just below the melting point.⁵¹ However, for supported clusters, interactions with the substrate may influence the behavior, and so these results may not reflect the intrinsic behavior of the isolated cluster.

Experimental evidence for structural transitions in isolated metal clusters is scarce. Ion mobility measurements have revealed some examples for both aluminum⁵³ and gold.⁵⁴ Low temperature dips in the heats capacities for $\text{Al}_{56}^+ - \text{Al}_{62}^+$ have been attributed to exothermic structural transitions (annealing).^{15,18}

II. EXPERIMENTAL METHODS

Heat capacities are measured using multicollision induced dissociation.^{11,55} Briefly, aluminum cluster ions are generated by pulsed laser vaporization of a liquid aluminum target in a helium buffer gas.⁵⁶ After formation the clusters are carried by the buffer gas flow into a 10 cm long temperature-variable extension where their temperature is set. The cluster cations that exit the extension are accelerated and focused into a quadrupole mass spectrometer where a specific cluster size is selected. The size-selected clusters are then focused into a collision cell containing 1 torr of helium. As the clusters enter the collision cell, they undergo numerous collisions with the helium buffer gas; each collision converts a small fraction of the cluster ion's translational energy into internal energy. If the cluster's initial translational energy is high enough, some of them are excited to the point where they dissociate. The products and undissociated clusters are analyzed by a second quadrupole mass spectrometer and the fraction of the clusters that dissociate is determined from the mass spectrum. Measurements are performed for several different initial translational energies and the translational energy that is required to dissociate 50% of the clusters (TE50%D) is determined from a linear regression. TE50%D is then measured as a function of the cluster's temperature. The derivative of the TE50%D with respect to temperature is proportional to the heat capacity. The proportionality constant depends on the fraction of the cluster ion's translational energy that is converted into internal energy, which is obtained from a simple impulsive collision model.⁵⁷

For the annealing studies, a temperature-variable annealing section is inserted between the source region and the temperature-variable extension.¹⁸ In the studies reported here, the clusters are annealed to 523 and 773 K before the

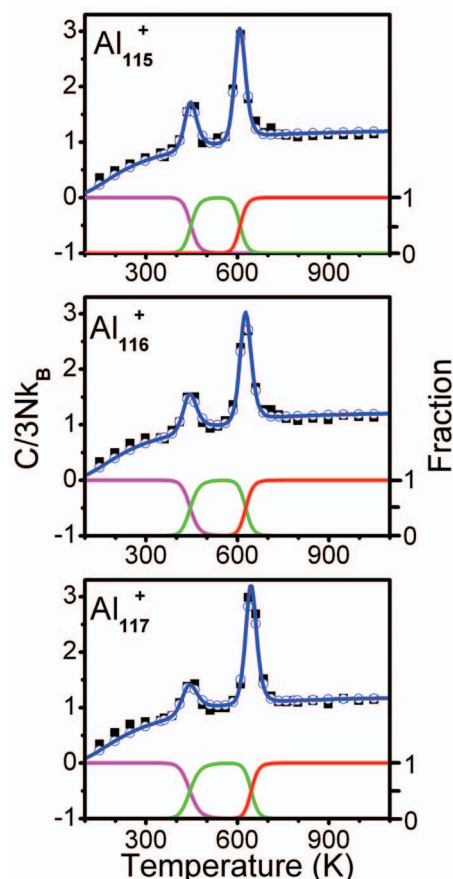


FIG. 1. Heat capacities measured as a function of temperature for Al_{115}^+ , Al_{116}^+ , and Al_{117}^+ . The filled black squares are the measured values. The heat capacities are plotted relative to the classical value $3Nk_B$, where $3N = 3n - 6 + 3/2$ and k_B is the Boltzmann constant. The open blue circles are a fit obtained using a three-state model using $\Delta T = 25$ K or 50 K (see text). The solid blue lines show heat capacities obtained from the fit with $\Delta T = 5$ K. The lines at the bottom of each plot show the relative abundances of the low energy structure (green), high energy structure (purple), and liquid (red) as a function of temperature (using the scale on the right hand axes).

heat capacity measurements are performed. The source region is kept at room temperature by means of a recirculating chiller.

III. EXPERIMENTAL RESULTS

Heat capacities measured as a function of temperatures for unannealed Al_{115}^+ , Al_{116}^+ , and Al_{117}^+ clusters are shown in Fig. 1. The filled squares are the experimental results. The open circles and the solid lines are fits to the measured points using a three-state model^{17,18,58} described in more detail below. The heat capacities are plotted in units of the classical value, $3Nk_B$, where $3N = (3n - 6 + 3/2)$ and k_B is the Boltzmann constant. All three clusters have two well-resolved peaks in their heat capacities. We have measured the heat capacities for larger Al_n^+ clusters with 100–128 atoms and only Al_{115}^+ , Al_{116}^+ , and Al_{117}^+ show the two well-resolved peaks. Note that the heat capacities were recorded with $\Delta T = 25$ K around the peaks and $\Delta T = 50$ K away from the peaks.

To better understand the origin of the two transitions observed in the heat capacities we performed some annealing experiments. After the clusters are generated at room tem-

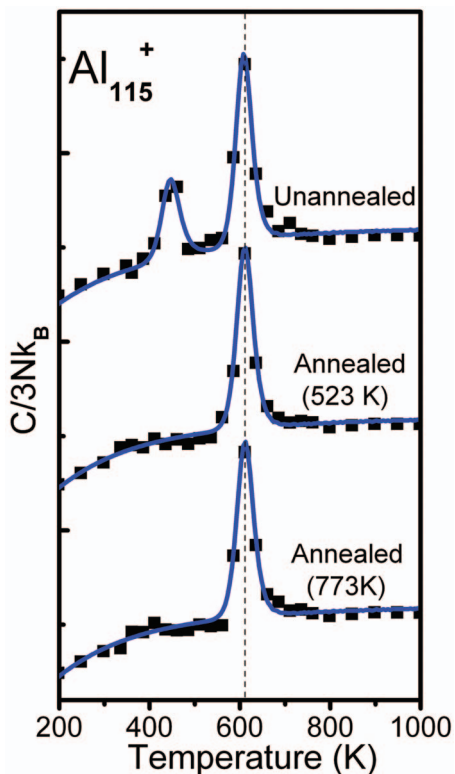


FIG. 2. Heat capacities recorded for Al_{115}^+ after annealing to 523 and 773 K (filled black squares). The heat capacities are plotted in units of $3Nk_B$, where $3N=3n-6+3/2$ and k_B is the Boltzmann constant. The heat capacities for unannealed Al_{115}^+ are included for comparison. The blue lines are fits to the experimental data values using two- and three-state models with $\Delta T=5$ K (see text).

perature in the source region, they are annealed to either 523 K (between the two peaks) or to 723 K (well above both peaks). The annealing results for Al_{115}^+ are shown in Fig. 2, where blue lines are fits to the experimental points (filled black squares). When annealed to either 523 or 723 K, the low temperature peak in the heat capacities disappears, but the higher temperature transition remains virtually unchanged in both position and size. The annealing results for Al_{116}^+ and Al_{117}^+ are exactly the same as for Al_{115}^+ .

IV. DISCUSSION

A. The origin of the two peaks

Excluding electronic effects, there are three possible causes for two peaks in the heat capacity: (1) partial melting, where the surface or some other part of the cluster melts at a lower temperature than the rest, (2) two structural isomers that melt at different temperatures, and (3) a solid-to-solid transition followed by melting. We will now consider each of these possible explanations in turn.

Surface premelting is a well-known phenomenon for bulk surfaces. It occurs if the surface energy γ_{SV} is greater than $\gamma_{SL} + \gamma_{LV}$ (where the subscripts S , L , and V are solid, liquid, and vapor). For aluminum, the compact Al(111) and Al(001) surfaces do not premelt,^{59,60} although the more open Al(110) does.^{59,61,62} For bulk surfaces the thickness of the premelted layer increases smoothly as the temperature approaches the bulk melting point, which leads to a low tem-

perature tail on the heat capacity peak due to bulk melting. In cluster simulations, the melting of just the surface layer can lead to a peak in the heat capacity at a temperature below the main melting transition. It is also feasible that some other subset of the atoms in the cluster could melt (i.e., become mobile) at a lower temperature than the rest of the cluster. However, it is difficult to reconcile the annealing results with premelting being the explanation for the low temperature peaks in the heat capacities. To account for the annealing results, it would be necessary for the premelted atoms not to refreeze when cooled to well below their melting temperature. The freezing of liquids can be kinetically hindered by the need to generate a critical nucleus to template the solid. However, it is difficult to imagine that the premelted atoms cannot refreeze when the rest of the cluster has already frozen, forming a nucleus. For this reason we rule out partial melting as the cause of the two features in the heat capacity plot.

We now consider the possibility that two structural isomers melting at different temperatures are responsible for the two peaks in the heat capacity. With this explanation, when the first isomer melts it cannot refreeze into the higher melting temperature isomer on the time scale of the experiment. However, we know from the annealing experiments that the higher temperature peak is recovered after annealing to 773 K (above both peaks). So clearly the liquid can freeze promptly into the higher melting temperature structure and so this cannot be the cause of the two peaks in the heat capacity.

We now consider the third option mentioned above: The low temperature peak in the heat capacity is due to a structural transition. Since we have ruled out cases (1) and (2) above, case (3) (a solid-to-solid transition from a low energy structure to a high energy structure followed by melting of the higher energy structure) is the most likely explanation for the two peaks observed in the heat capacities for Al_{115}^+ , Al_{116}^+ , and Al_{117}^+ . There are two distinct mechanisms for the structural transition: Either it occurs through a liquid intermediate or directly from solid to solid. In the former, there are two isomers that melt at different temperatures, and when the low-melting temperature isomer melts it quickly refreezes into the high-melting temperature isomer. This process leads to a peak or dip in the heat capacity with an area proportional to the enthalpy difference between the two states. The fact that there is a peak in the heat capacity indicates that the high-melting temperature isomer has a higher enthalpy than the low-melting temperature one, and so the structural transition is driven by entropy. In the scenario outlined above the solid-to-solid transition occurs with the liquid as an intermediate. There is evidence for this type of process from simulations.^{37,40,43} However, the solid-to-solid transition could also occur directly (i.e., without a liquid intermediate). The heat capacity signature for a direct solid-to-solid transition is indistinguishable from one that proceeds through a liquid intermediate; in both cases the area of the peak reflects the enthalpy difference between the two solid states.

B. Fitting the results with a three-state model

A solid-to solid transition followed by melting can be represented by



where C_{LE} and C_{HE} are the low energy and high energy solids, respectively, and L is the liquid. In previous work we have developed a three-state model that can be used to fit the heat capacities for a system melting through an intermediate as in Eq. (1).^{17,18,58} We assume that melting occurs in the dynamic phase coexistence regime, where the transition is between fully solid and fully liquid clusters (i.e., there are no partially melted intermediates). This behavior was first observed in simulations.^{63–70} There is now experimental evidence for dynamic phase coexistence for aluminum clusters in the size range examined here.⁷¹ In this limit the melting transition can be described by an equilibrium constant given by

$$K_M(T) = \exp\left[\frac{-\Delta H_M}{R}\left(\frac{1}{T} - \frac{1}{T_M}\right)\right], \quad (2)$$

where K_M , ΔH_M , and T_M are the equilibrium constant, enthalpy change (latent heat), and transition temperature (where the amounts of the high enthalpy solid and liquid are equal). If we also assume that the solid-to-solid transition occurs under equilibrium [as indicated in Eq. (1)], the equilibrium constant for this process can be written as

$$K_{SS}(T) = \exp\left[\frac{-\Delta H_{SS}}{R}\left(\frac{1}{T} - \frac{1}{T_{SS}}\right)\right], \quad (3)$$

where K_{SS} , ΔH_{SS} , and T_{SS} are the equilibrium constant, enthalpy change, and transition temperature (where the amounts of high enthalpy and low enthalpy solids are equal) for the solid-to-solid transition. The contributions of the enthalpy changes for the two transitions to the internal energy and to the heat capacity are

$$E_{IE}(T) = (f_{SHE}(T) + f_L(T))\Delta H_{SS} + f_L(T)\Delta H_M, \quad (4)$$

$$C(T) = \frac{dE_{IE}(T)}{dT} = \frac{\Delta[(1 - f_{SLE}(T))\Delta H_{SS} + f_L(T)\Delta H_M]}{\Delta T}, \quad (5)$$

where $f_{SLE}(T)$, f_{SHE} , and $f_L(T)$ are the fractions of the low energy solid, the high energy solid, and the liquid present at temperature T . We add this to the component of the heat capacity due to the internal energy of the solid and liquid clusters. For both solids and the liquid we use the heat capacity derived from the modified Debye model⁵⁸ multiplied by scaling factors. The simulation is fit to the measured heat capacities using a least-squares procedure with seven adjustable parameters: ΔH_{SS} , T_{SS} , ΔH_M , T_M , S_{LE} , S_{HE} , and S_L , where the final three are the scale factors. More details are given in Refs. 17 and 18. The unfilled circles in Fig. 1 show the result of this fit with the same values for ΔT as used in the experiments ($\Delta T=25$ K close to the peaks and 50 K away from the peaks). The fits to the experimental data for both peaks are very good. In both cases it appears that the width of the transition is reproduced. The solid blue line

TABLE I. Parameters derived for the structural transitions and melting transitions for Al_{115}^+ , Al_{116}^+ , and Al_{117}^+ by fitting the measured heat capacities with a three-state model (see text).

Cluster	Structural transition		Melting transition	
	T_{ST} (K)	ΔH_{ST} (kJ mol ⁻¹)	T_M (K)	ΔH_M (kJ mol ⁻¹)
Al_{115}^+	448	126.0	609	265.3
Al_{116}^+	445	112.1	627	270.9
Al_{117}^+	445	98.9	646	291.9

going through the data in Fig. 1 shows the result of a simulation with $\Delta T=5$ K. The calculated heat capacities obtained with 5 K and 25 K or 50 K are similar, indicating that the value of ΔT used in the experiments is small enough that the peaks are not significantly broadened. The lines beneath each heat capacity plot show the amount of low energy solid, high energy solid, and liquid present at each temperature.

In the three-state model used to fit the measured heat capacities we assume that both processes occur under equilibrium. While this appears to be true for the melting transition, it is not true for the solid-to-solid transition, because the low energy structure is not recovered from the high energy structure after annealing. It follows that the solid-to-solid transition requires a superheated solid to occur on the experimental timescale, and the equilibrium transition temperature is below the peak in the heat capacity. The enthalpy change associated with transition can still be determined from the peak in the heat capacity (the enthalpy change is the area under the peak). Despite the fact that the transition does not occur under equilibrium, the three-state model still provides a good fit to the measured peak in the heat capacity for the solid-to-solid transition, and so the enthalpy changes shown in Table I for the solid-to-solid transition are reliable.

The enthalpy changes for the structural transitions are around 100–125 kJ mol⁻¹ and decrease slightly with increasing cluster size. The enthalpy changes for the melting transitions are around 2.5–3.0 times larger than for the structural transitions and increase slightly with increasing cluster size. The sum of the enthalpy changes (structural transition plus melting) for each cluster is almost independent of cluster size (380–390 kJ mol⁻¹).

C. Origin of the low energy structure observed for unannealed clusters

The low energy structure responsible for the low temperature peak in the heat capacities for Al_{115}^+ , Al_{116}^+ , and Al_{117}^+ cannot be accessed from the liquid or from the high enthalpy structure on the timescale of our experiments and so these clusters have hidden ground states. If the low energy structure cannot be accessed from other structures or the liquid on our experimental timescale, where does it come from for the unannealed clusters? One possible explanation is that the low energy structure observed for Al_{115}^+ , Al_{116}^+ , and Al_{117}^+ clusters is generated by epitaxy on smaller clusters, where the smaller clusters act as a nucleus and follow a growth pattern that provides access to the low energy structure. For this to occur, the temperature of the cluster must

remain below the temperature of the structural transition (the peak in the heat capacity) during the last stages of cluster growth. Adding an atom to a growing cluster adds an amount of energy equal to the dissociation energy. This energy, when distributed, will transiently heat the cluster before being removed by collisions with the buffer gas. The dissociation energies of clusters in the size range considered here are around 3 eV.¹⁹ Adding this much energy to Al_{115}^+ causes the temperature to increase by around 100 K (assuming a classical heat capacity). The cluster growth region of the source is kept at close to room temperature and so the peak temperature achieved for the clusters during cluster growth is around 400 K (assuming that the clusters cool down completely before the addition of another atom). 400 K is just below the low temperature peaks in the heat capacity, so it is plausible for the clusters to grow without converting into the higher energy structure.

V. SUMMARY AND CONCLUSIONS

At least three states are important for Al_{115}^+ , Al_{116}^+ , and Al_{117}^+ clusters: A low enthalpy structure, a high enthalpy structure, and a liquidlike state. When cooled, the liquidlike state freezes exclusively into the high enthalpy structure, which does not convert into the low enthalpy structure on our experimental timescale. However, the low enthalpy structure is observed for unannealed clusters, where it is believed to have been generated by epitaxy on smaller clusters. The results presented here provide no insight into the nature of the high and low energy structures. It is possible that the unusual behavior observed for Al_{115}^+ , Al_{116}^+ , and Al_{117}^+ (these are the only clusters that show two well-resolved peaks in their heat capacities) occurs because there is a basic change in the ground state structure in this size regime.

ACKNOWLEDGMENTS

We gratefully acknowledge the support of the National Science Foundation (CHE0616564 and CHE0911462).

- ¹M. Schmidt, R. Kusche, W. Kronmüller, B. von Issendorff, and H. Haberland, *Phys. Rev. Lett.* **79**, 99 (1997).
- ²M. Schmidt, R. Kusche, B. von Issendorff, and H. Haberland, *Nature (London)* **393**, 238 (1998).
- ³M. Schmidt, R. Kusche, T. Hippler, J. Donges, W. Kronmüller, B. von Issendorff, and H. Haberland, *Phys. Rev. Lett.* **86**, 1191 (2001).
- ⁴M. Schmidt and H. Haberland, *C. R. Phys.* **3**, 327 (2002).
- ⁵M. Schmidt, J. Donges, Th. Hippler, and H. Haberland, *Phys. Rev. Lett.* **90**, 103401 (2003).
- ⁶H. Haberland, T. Hippler, J. Donges, O. Kostko, M. Schmidt, and B. von Issendorff, *Phys. Rev. Lett.* **94**, 035701 (2005).
- ⁷F. Chiro, P. Feiden, S. Zamith, P. Labastie, and J. M. L'Hermite, *J. Chem. Phys.* **129**, 164514 (2008).
- ⁸C. Hock, S. Strassburg, H. Haberland, B. von Issendorff, A. Aguado, and M. Schmidt, *Phys. Rev. Lett.* **101**, 023401 (2008).
- ⁹A. A. Shvartsburg and M. F. Jarrold, *Phys. Rev. Lett.* **85**, 2530 (2000).
- ¹⁰G. A. Breaux, C. M. Neal, B. Cao, and M. F. Jarrold, *Phys. Rev. B* **71**, 073410 (2005).
- ¹¹G. A. Breaux, R. C. Benirschke, T. Sugai, B. S. Kinnear, and M. F. Jarrold, *Phys. Rev. Lett.* **91**, 215508 (2003).
- ¹²G. A. Breaux, D. A. Hillman, C. M. Neal, R. C. Benirschke, and M. F. Jarrold, *J. Am. Chem. Soc.* **126**, 8628 (2004).
- ¹³G. A. Breaux, B. Cao, and M. F. Jarrold, *J. Phys. Chem. B* **109**, 16575 (2005).

- ¹⁴G. A. Breaux, R. C. Benirschke, and M. F. Jarrold, *J. Chem. Phys.* **121**, 6502 (2004).
- ¹⁵G. A. Breaux, C. M. Neal, B. Cao, and M. F. Jarrold, *Phys. Rev. Lett.* **94**, 173401 (2005).
- ¹⁶C. M. Neal, A. K. Starace, M. F. Jarrold, K. Joshi, S. Krishnamurty, and D. G. Kanhere, *J. Phys. Chem. C* **111**, 17788 (2007).
- ¹⁷C. M. Neal, A. K. Starace, and M. F. Jarrold, *Phys. Rev. B* **76**, 054113 (2007).
- ¹⁸M. F. Jarrold, B. Cao, A. K. Starace, C. M. Neal, and O. H. Judd, *J. Chem. Phys.* **129**, 014503 (2008).
- ¹⁹A. K. Starace, C. M. Neal, B. Cao, M. F. Jarrold, A. Aguado, and J. M. López, *J. Chem. Phys.* **129**, 144702 (2008).
- ²⁰W. Zhang, F. Zhang, and Z. Zhu, *Phys. Rev. B* **74**, 033412 (2006).
- ²¹Z. H. Li and D. G. Truhlar, *J. Am. Chem. Soc.* **130**, 12698 (2008).
- ²²P. J. Hsu, J. S. Luo, S. K. Lai, J. F. Wax, and J.-L. Bretonnet, *J. Chem. Phys.* **129**, 194302 (2008).
- ²³J. G. O. Ojwang, R. van Santen, G. J. Kramer, A. C. T. van Duin, and W. A. Goddard, *J. Chem. Phys.* **129**, 244506 (2008).
- ²⁴S. M. Ghazi, S. Zorriasatein, and D. G. Kanhere, *J. Phys. Chem. A* **113**, 2659 (2009).
- ²⁵V. V. Nauchitel and A. J. Pertsin, *Mol. Phys.* **40**, 1341 (1980).
- ²⁶H.-P. Cheng and R. S. Berry, *Phys. Rev. A* **45**, 7969 (1992).
- ²⁷A. Aguado, J. M. López, J. A. Alonso, and M. J. Stott, *J. Chem. Phys.* **111**, 6026 (1999).
- ²⁸F. Calvo and F. Spiegelmann, *J. Chem. Phys.* **112**, 2888 (2000).
- ²⁹Y. J. Lee, E.-K. Lee, S. Kim, and R. M. Nieminen, *Phys. Rev. Lett.* **86**, 999 (2001).
- ³⁰A. Aguado, L. M. Molina, J. M. López, and J. A. Alonso, *Eur. Phys. J. D* **15**, 221 (2001).
- ³¹K. Joshi, D. G. Kanhere, and S. A. Blundell, *Phys. Rev. B* **67**, 235413 (2003).
- ³²F. Calvo and F. Spiegelmann, *J. Chem. Phys.* **120**, 9684 (2004).
- ³³A. Aguado, *J. Phys. Chem. B* **109**, 13043 (2005).
- ³⁴A. Aguado and J. M. López, *Phys. Rev. B* **74**, 115403 (2006).
- ³⁵C. Hock, C. Bartels, S. Straßburg, M. Schmidt, H. Haberland, B. von Issendorff, and A. Aguado, *Phys. Rev. Lett.* **102**, 043401 (2009).
- ³⁶A. Ghazali and J.-C. S. Lévy, *Phys. Lett. A* **228**, 291 (1997).
- ³⁷C. L. Cleveland, W. D. Luedtke, and U. Landman, *Phys. Rev. Lett.* **81**, 2036 (1998).
- ³⁸A. Pundt, M. Dornheim, M. Guerdane, H. Teichler, H. Ehrenberg, M. T. Reetz, and N. M. Jisrawi, *Eur. Phys. J. D* **19**, 333 (2002).
- ³⁹T. X. Li, S. M. Lee, S. J. Han, and G. H. Wang, *Phys. Lett. A* **300**, 86 (2002).
- ⁴⁰D. Schebarchov and S. C. Hendy, *Phys. Rev. Lett.* **95**, 116101 (2005).
- ⁴¹C.-L. Kuo and P. Clancy, *J. Phys. Chem. B* **109**, 13743 (2005).
- ⁴²Z. Zhang, W. Hu, and S. Xiao, *Phys. Rev. B* **73**, 125443 (2006).
- ⁴³D. Schebarchov and S. C. Hendy, *Phys. Rev. B* **73**, 121402(R) (2006).
- ⁴⁴J. P. K. Doye and D. J. Wales, *Phys. Rev. Lett.* **80**, 1357 (1998).
- ⁴⁵J. P. K. Doye and F. Calvo, *J. Chem. Phys.* **116**, 8307 (2002).
- ⁴⁶V. A. Mandelshtam, P. A. Frantsuzov, and F. Calvo, *J. Phys. Chem. A* **110**, 5326 (2006).
- ⁴⁷E. G. Noya and J. P. K. Doye, *J. Chem. Phys.* **124**, 104503 (2006).
- ⁴⁸V. A. Mandelshtam and P. A. Frantsuzov, *J. Chem. Phys.* **124**, 204511 (2006).
- ⁴⁹V. A. Sharapov and V. A. Mandelshtam, *J. Phys. Chem. A* **111**, 10284 (2007).
- ⁵⁰L. Zhan, J. Z. Y. Chen, and W. K. Liu, *J. Chem. Phys.* **127**, 141101 (2007).
- ⁵¹K. Koga, T. Ikeshoji, and K. Sugawara, *Phys. Rev. Lett.* **92**, 115507 (2004).
- ⁵²D. Zanchet, B. D. Hall, and D. Ugarte, *J. Phys. Chem. B* **104**, 11013 (2000).
- ⁵³M. F. Jarrold and J. E. Bower, *J. Chem. Phys.* **98**, 2399 (1993).
- ⁵⁴P. Weis, T. Bierweiler, E. Vollmer, and M. M. Kappes, *J. Chem. Phys.* **117**, 9293 (2002).
- ⁵⁵C. M. Neal, A. K. Starace, and M. F. Jarrold, *J. Am. Soc. Mass Spectrom.* **18**, 74 (2007).
- ⁵⁶C. M. Neal, G. A. Breaux, B. Cao, A. K. Starace, and M. F. Jarrold, *Rev. Sci. Instrum.* **78**, 075108 (2007).
- ⁵⁷M. F. Jarrold and E. C. Honea, *J. Phys. Chem.* **95**, 9181 (1991).
- ⁵⁸D. Poland, *J. Chem. Phys.* **126**, 054507 (2007).
- ⁵⁹A. W. D. van der Gon, R. J. Smith, J. M. Gay, D. J. O'Connor, and J. F. van der Veen, *Surf. Sci.* **227**, 143 (1990).
- ⁶⁰A. M. Molenbroek and J. W. M. Frenken, *Phys. Rev. B* **50**, 11132 (1994).

- ⁶¹ P. von Blanckenhagen, W. Schommers, and V. Voegelé, *J. Vac. Sci. Technol. A* **5**, 649 (1987).
- ⁶² P. Stoltze, J. K. Nørskov, and U. Landman, *Surf. Sci.* **220**, L693 (1989).
- ⁶³ C. L. Briant and J. J. Burton, *J. Chem. Phys.* **63**, 2045 (1975).
- ⁶⁴ R. S. Berry, J. Jellinek, and G. Natanson, *Phys. Rev. A* **30**, 919 (1984).
- ⁶⁵ T. L. Beck, J. Jellinek, and R. S. Berry, *J. Chem. Phys.* **87**, 545 (1987).
- ⁶⁶ H. Reiss, P. Mirabel, and R. L. Whetten, *J. Phys. Chem.* **92**, 7241 (1988).
- ⁶⁷ P. Labastie and R. L. Whetten, *Phys. Rev. Lett.* **65**, 1567 (1990).
- ⁶⁸ H.-P. Cheng, X. Li, R. L. Whetten, and R. S. Berry, *Phys. Rev. A* **46**, 791 (1992).
- ⁶⁹ J. P. Rose and R. S. Berry, *J. Chem. Phys.* **98**, 3246 (1993).
- ⁷⁰ B. Vekhter and R. S. Berry, *J. Chem. Phys.* **106**, 6456 (1997).
- ⁷¹ B. Cao, A. K. Starace, O. H. Judd, and M. F. Jarrold, *J. Chem. Phys.* **130**, 204303 (2009).